Enabling High-Temperature Superconducting Technologies Toward Practical Applications

Jian X. Jin, Ying Xin, Qiu L. Wang, Yu S. He, Chuan B. Cai, Yin S. Wang, and Zan M. Wang

(Invited Paper)

***Abstract*—This work covers the high-temperature superconducting (HTS) technologies based on the highlights in recent achievements in the applied HTS field in China. Its comprehensive coverage includes practical HTS material manufacturing and characterization, large-scale applications, and electronic applications. The applied HTS technologies have been well enabled to build applicable devices, and their characteristics have been well verified in the HTS devices developed to be industrialized for practical applications. The highlighted HTS devices and their performance details reveal the trend and the necessary improvement required to reach the goal of industrial applications of HTS technologies.**

***Index Terms*—High-temperature (T_c) superconductor (HTS), HTS cable, HTS electronic device, HTS fault-current limiter, HTS large-scale application, HTS magnet, HTS measurement technique, HTS motor, HTS MRI, HTS strong current device, HTS transformer, HTS 2G wire.**

I. Introduction

In RECENT years, the applied high-temperature superconducting (HTS) technology has been well enabled in all principal aspects and gradually approaches its era of industrialization. There has been a trend of increasing industry involvement in HTS application R&D projects in China in the last few years, which has positively driven the HTS R&D activities to the road of practical applications. To reflect the progress, the applied HTS developments inside China is summarized which can be categorized and includes principally:

1) HTS electric power devices and applications;
2) HTS machine and magnet applications;
3) HTS electronic devices and applications;
4) HTS materials' production;
5) HTS characterization techniques.

Highlights of those projects and activities will be revealed, and from which HTS performances will be verified and identified in the practical devices developed to further enable the HTS technologies for industrial applications.

Manuscript received June 15, 2014; accepted July 29, 2014. Date of publication August 8, 2014; date of current version September 11, 2014.

J. X. Jin is with the School of Electrical Engineering and Automation,Tianjin University, Tianjin 300072, China (e-mail: jjin12203@yahoo.com).

Y. Xin is with the Center of Applied Superconductivity, School of Electrical Engineering and Automation, Tianjin University, Tianjin 300072, China.

Q. L. Wang is with the Division of Superconducting Science and Technology, Institute of Electrical Engineering, Chinese Academy of Sciences, Beijing 100190, China.

Y. S. He is with the Institute of Physics, Chinese Academy of Sciences, Beijing 100190, China.

C. B. Cai is with the Research Center for Superconductors and Applied Technologies, Physics Department, Shanghai University, Shanghai 200444, China.

Y. S. Wang is with the State Key Laboratory for Alternate Electrical Power System with Renewable Energy Sources, Key Laboratory of HV and EMC Beijing, North China Electric Power University, Beijing 102206, China.

Z. M. Wang is with Alltech Medical Systems, Chengdu 611731, China.

Color versions of one or more of the figures in this paper are available online at http://ieeexplore.ieee.org.

Digital Object Identifier 10.1109/TASC.2014.2346496

II. HTS Electrical Applications

A. HTS Fault Current Limiters

Development of a saturated iron-core-type superconducting fault-current limiter (SISFCL) has been the R&D focus of Innopower Superconductor Cable Co., Ltd. (Innopower) since 2004 [1]. Intensive studies, theoretical analysis, computer simulation, and experiments have been carried out to further understand the functional characteristics of this kind of device in normal power transmission and fault-current limiting operation.

Fabrication techniques in large-size HTS coil winding, electrical insulation, joint, and configuration of the coils, among others, have been developed for the superconducting dc coil. Difficulties in the unconventional design and manufacture of the copper ac coils and oil tanks have also been overcome. Innovative approaches in the iron-core design improve the performance of the device, ensuring very low impedance during normal power transmission and adequately high impedance for fault-current limiting. The dc bias magnetization circuit control and addition of the voltage suppression and energy release unit make the device more reliable in grid operation [2], [3].

Practical SISFCL Devices:

1) A 35-kV/90-MVA SISFCL was installed at the Puji substation of China Southern Power Grid in Kunming at the end of 2007. Performances in normal power transmission and during fault-current limiting operation have been satisfactory, showing a good agreement with design expectations [4]–[7].
2) A 220-kV/300-MVA 3-phase SISFCL was installed at Shigezhuang substation of China State Grid in Tianjin in 2012 [8], [9]. Its fault-current limiting capacity has not been fully tested yet due to the grid condition. Fig. 1 shows the 35-kV and 220-kV devices at their installation sites, which specifications are shown in Table I.
3) A 500-kV with normal transmission current rated 3.15-kA single-phase SISFCL prototype is under development. After viability of this prototype is verified by comprehensive factory testing and optimization, three

(a)

(b)

Fig. 1. 35-kV/90-MVA SISFCL (a) and the 220-kV/300-MVA SISFCL (b) at their installation sites.

TABLE I
SPECIFICATIONS OF THE 90-MVA AND 300-MVA SISFCLS

Rated power	90 MVA	300 MVA
Rated voltage	35 kV	220 kV
Rated current	1.5 kA	0.8 kA
Max. expected fault current	41 kA	50 kA
Max. limited current	20 kA	30 kA
Restoration time	< 800 ms	< 500 ms
Total weight	27 ton	120 ton

single-phase units will be manufactured and installed in the heavily populated Pearl River Delta area in the China Southern power grid.

The HTS wires used for these SISFCL were BSCCO 2223 ($Bi_2Sr_2Ca_2Cu_3O_{10+\delta}$ or Bi-2223/Ag) 1G multifilament tapes. Since the dc bias coil where the HTS wires are used will be mainly exposed to a parallel magnetic field with strength in a range of 0.1–0.3 T, the BSCCO 2223 tapes operated in liquid nitrogen (LN_2) can function sufficiently and safely for this kind of device. The use of BSCCO 2223 tapes instead of the YBCO ($YBa_2Cu_3O_{7-\delta}$ or Y-123) 2G coated tapes in this case is more cost effective at present.

The SISFCL is promising for industrial applications, particularly for high-voltage power grids to assist utilities to cope with the ever growing and challenging short-circuit problems.

Various HTS FCL Devices:

1) A 10.5-kV/1.5-kA 3-phase-bridge-type SFCL was fabricated by the Institute of Electrical Engineering, Chinese Academy of Sciences (IEE CAS) in 2004 [10]. The HTS coils used were structured in double pancakes. Four double pancakes at each end of the coil were wound with two parallel BSCCO 2223 tapes, and other six double pancakes in the coil were wound with single tapes. This device was installed and tested in a real power grid in Loudi of Hunan and then moved to the superconducting substation in Baiyin of Gansu for demonstration.
2) A 10-kV/200-A resistive-type SFCL prototype using YBCO 2G tapes was built and tested in 2012 by the Shanghai Jiaotong University [11]. This FCL consisted of several current limiting modules connected in series, each module is able to withstand 700–800 V during faults. It was able to reduce fault currents by 30%–70% of the original values depending on the shunt resistors used. YBCO tapes used were prepared by the Shanghai Jiaotong University. The tape had Ni-W substrate and 20-μm copper stabilizers on both sides. The superconducting layer was fabricated using the pulse laser deposition (PLD) method.
3) Other developed SFCL prototypes include: i) 100-kJ/1-kA/20-kVA superconducting fault-current limiter magnetic energy storage (SFCL-MES) was built and tested by the IEE CAS in 2006 [12]. ii) Following the original development of the SISFCL [13] a hybrid SFCL with the combination of an HTS saturable reactor [14] and an HTS resistive limiter [15], a dc transmission-cable-type SFCL, and also a power electronic hybrid-bridge-type SFCL [16] have been proposed, analyzed and tested by the research group from the University of Electronic Science and Technology of China (UESTC).

B. HTS Cables and Transmission

1) 3-phase, 35-kV/2.5-kA/121-MVA/33.5-m HTS ac power cable, is the first Chinese HTS power transmission cable installed in a real power grid having a warm dielectric cable system [17], [18]. This system was activated successfully at the Puji Substation of China Southern Power Grid in 2004 and stopped operation in 2011 due to the cable's cryogenic system reaching its designed lifespan. The 35-kV cable system had delivered more than 800 000 000 kWh of electricity to 4 industrial customers (including 2 metallurgical refineries) and about 100 000 residential customers before its operation was suspended. The system consisted of three 33.5-m cables, six terminations, and one closed-cycle liquid nitrogen cooling station. The cable was constructed using a round corrugated stainless steel tube and helically wrapping layers of BSCCO 2223 multifilament tapes supplied by the Innova Superconductor Technology Co., Ltd. (InnoST). The installation for the 35-kV HTS power cable is shown in Fig. 2.
2) 3-phase, 10.5-kV/1.5-kA/22-MVA/75-m HTS ac power cable prototype, was developed by the IEE CAS, which was installed and operated in a distribution grid of the Changtong Power Cable Factory in Gansu at the end of 2004 [19]. Each cable consists of 36 BSCCO 2223 tapes from the American Superconductor Corporation (AMSC) spirally reeled into two layers on the corrugated pipe and soldered to the copper terminals by low-melting-point alloy solder.
3) 1.3-kV/10-kA/13-MVA/360-m HTS dc cable prototype, was developed and tested by the IEE CAS in 2012 [20]. The cable was used to connect the substation and the bus bar of an aluminum electrolyzing workshop in the Zhongfu Industrial Co., Ltd. in Henan. The HTS conductor consisted of 5 layers of BSCCO 2223 tapes, in which one layer was fabricated with the tapes from

(a)

(b)

Fig. 2. 35-kV HTS ac power cable system (a) and its terminal (b).

TABLE II
SPECIFICATIONS OF THE SMES DEVICES IN THE IEE CAS

Capacity	17 kJ [23]	30 kJ [24]	100 kJ [12]	1 MJ [25]	2 MJ [26]
Current	86 A	155 A	1 kA	564 A	490 A
Inductance	4.7 H	2.5 H	0.2 H	6.3 H	16.6 H
Wire	Bi-2223	Bi-2223	NbTi	Bi-2223	NbTi
Cooling method	GM cooler (10 K)	GM cooler (20 K)	GM cooler (4.2 K)	GM cooler (4.2 K)	GM cooler (4.2 K)

the InnoST and four layers were fabricated with the tapes from the Sumitomo Electric Industries.

4) Various HTS cable and transmission technologies also include: i) dc cable and transmission; ii) double functional cable; iii) smart power transmission and system. The UESTC has built the above three cable models with application techniques, and developed the steady and dynamic theoretical models of HTS dc power transmission aiming for the potential applications in dc transmissions and smart grids [21], [22]. The HTS dc cable allows power transmission at a substantially reduced voltage level with a fault safe function, eliminating the need of very high voltage insulation and transformers.

C. HTS SMES

1) The IEE CAS built a number of superconducting magnetic energy storage (SMES) prototypes using HTS wires or low temperature superconductor (LTS) wires for laboratory investigation or testing in power networks. Their main specifications are shown in Table II. Fig. 3 shows the IEE CAS' 1-MJ/0.5-MVA SMES system.
2) The Huazhong University of Science and Technology (HUST) developed a 35-kJ/7-kVA/100-A movable SMES prototype in 2005 [27]. The SMES magnet wound by BSCCO 2223 tapes was cooled by a GM cryocooler at

Fig. 3. 1-MJ/0.5-MVA SMES.

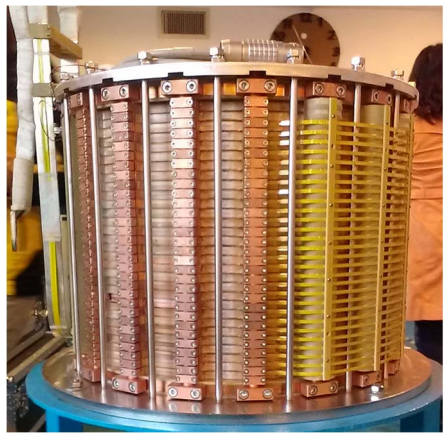

Fig. 4. HTS SMES coil.

20 K. Field experiments were carried out in the Laohukou Hydro Power Plant in Hubei province of China.

3) The Tsinghua University and the Tianwei Electric Group jointly developed a 300-kJ/150-kVA/600-A SMES prototype in 2004 [28]. The SMES magnet consisted of two coaxial solenoids wound with NbTi wires. The prototype used current-source-type circuit topology and was verified to compensate power system voltage sags.
4) The Chinese Electric Power Research Institute (CEPRI) developed a SMES prototype using YBCO tapes [29]. The system stored 0.38 kJ at 77 K and 3.42 kJ at 64 K, which can compensate a voltage sag in a power system.
5) The UESTC and the Innopower have jointly developed a SMES device to build a SMES energy exchange platform [30]. Fig. 4 shows the HTS SMES coil fabricated in the Innopower in 2013. A new bridge-type chopper formed by four MOSFETs has been built and studied. A SMES digitalization method has been developed with its digital control circuit built. The test results have shown a higher operation efficiency achieved when the new chopper is compared to the conventional chopper.

D. HTS Transformers

1) Based on their earlier experience of a 3-phase 26-kVA/0.4-kV/0.016-kV HTS transformer [31] and a 1-phase 45-kVA/2.4-kV/0.16-kV HTS transformer [32], the Tebian Electric Company (TBEA) and the IEE CAS designed and fabricated a 3-phase 630-kVA HTS power transformer in 2005, in which the primary and secondary

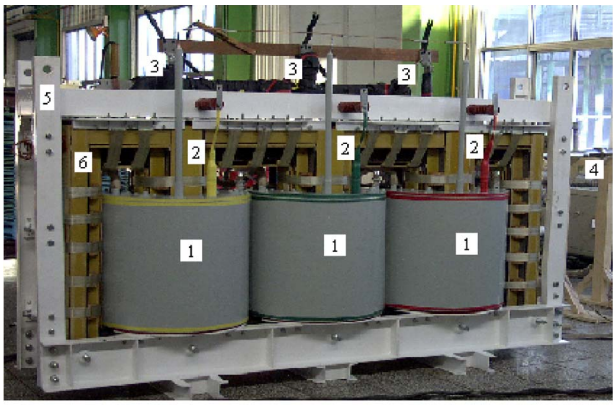

1-FGRP Dewar, 2-HV lead, 3-LV lead, 4-LN_2 pipe, 5-Clamp, 6-Core.

Fig. 5. 630-kVA three-phase transformer.

TABLE III
SPECIFICATIONS OF THE HTS TRANSFORMERS

Phase	3	1
Rated power	630 kVA	300 kVA
Voltage (prim. / sec.)	10.5 kV / 0.4 kV	25 kV / 0.86 kV
Current (prim. / sec.)	34.6 A / 909.3 A	12 A / 349 A
Wire	Bi-2223	Bi-2223
Cooling method	LN_2 (77 K)	LN_2 (67-77 K)

voltages and currents are 10.5-kV/0.4-kV and 34.6 A/909.3 A, respectively [33]. The 630-kVA HTS power transformer was installed and operated in a real power grid in Changji of Xinjiang, as shown in Fig. 5.

The windings are wound by strands of two parallel transposed hermetic stainless steel-enforced multifilamentary BSCCO 2223 tapes fabricated by the AMSC. Its convoluted amorphous alloy core has 5 limbs for 3 phases. The primary winding is a solenoid formed by 8 coil layers, and the secondary winding consists of 23 double pancakes connected in parallel. The windings are cooled by liquid nitrogen in cryostats having vacuum insulated fiberglass reinforced plastics (FGRP) with a diameter of 410 mm room temperature bore for the commercial amorphous alloy core having a diameter of 396 mm. In rated operation, the total ac loss in the three phase winding was 110.7 W excluding loss in current leads, which is qualitatively in agreement with the calculated result of 121.8 W. The hysteretic loss dominates the total loss; the sum of coupling loss and eddy-current loss is smaller than 9% of the hysteretic loss at the rated condition. The total efficiency of the transformer is 98.1%.

2) The Zhouzhu Locomotive Company developed a single-phase 300-kVA/25-kV/0.8-kV HTS traction transformer in 2005 to investigate the possibility of using a HTS transformer as an alternative in an electric locomotive [34]. Its efficiency is up to 99.87% when the cryogenic loss is excluded. Key specifications for the two aforementioned 630-kVA and 300-kVA HTS transformers are listed in Table III.
3) Special HTS transformers, such as an ultrahigh-current type and an ultrahigh-voltage type, were proposed by the UESTC group and patented, and a 1-MVA HTS transformer project has been established with industrial support from the Shuangxing Transformer Co., Ltd..

TABLE IV
SPECIFICATIONS OF THE 10-MW AND 12-MW WIND GENERATORS

Item	DEC	HUST
Rated power	10 MW	12 MW
Rated voltage	3.5 kV	3.3 kV
Rated current	840 A	2100 A
Rated speed	11 rpm	9 rpm
Rated frequency	2 Hz	3 Hz
Phase	6	3
Air-gap magnetic field	2 T	2.2 T
Operation temperature	20 K	4.2 K

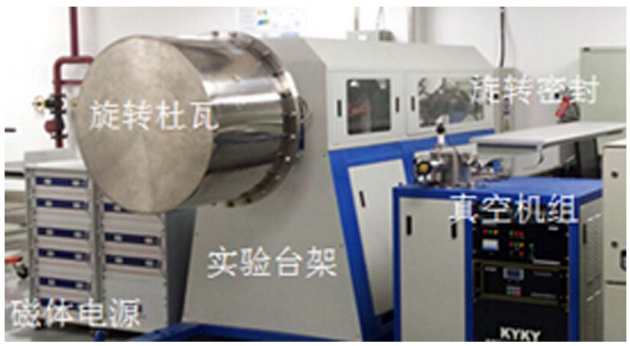

Fig. 6. Experimental wind generator prototype.

E. HTS Generators

1) A project to develop a 10-MW HTS wind generator has been launched by the Dongfang Electric Corporation (DEC) [35], [36] as its parameters shown in Table IV. An experimental prototype as shown in Fig. 6 has been built and tested, which uses 2G tape coils with direct conduction cooling to 30 K with cryocoolers. A novel structure of the proposed "YBCO + MgB_2 combined field coil" benefits from the advantage of the two types of superconducting materials' preferable performance at low field and high field, respectively. The capital cost of the whole field coil is verified to be significantly reduced with this approach.
2) Recently, in another newly started project led by HUST, topology of "outer armature rotating/static field winding" in a 12-MW LTS wind generator has been presented with design details also shown in the Table IV [37]. This structure removes the cryogenic rotary joints and simplifies the refrigeration system. The torque tube structure has a capacity of 56 MN. The torque load is about 14 MN at steady state and 40 MN under extreme conditions. Some key specifications of the 12-MW superconducting wind generator are also included.

III. HTS MACHINES AND APPLICATIONS

A. Superconducting Rotating Machines

1) In 2012, the China Shipbuilding Industry Corporation (CSIC) developed and tested a 1-MW HTS motor for the potential use in ship propulsion, as shown in Fig. 7

Fig. 7. 1-MW HTS motor prototype.

[38]. The HTS rotor system consisted of HTS field coils, refrigeration module cooled by He gas, cryostat, magnetic shield and support structure. There were six HTS field coils in the rotor wound with BSCCO 2223 wires operated at 35–40 K. The rated rotating speed was 1000 rpm and the efficiency at full load reached 95%. The whole stator system consisted of stator windings wound with improved copper wires, engine base, stator winding stand, bearing and chassis. The structure of stator tooth was an air-core type. The copper windings in the stator were cooled by chilled water.

2) In 2004, the IEE CAS made a 2-pole 150-W reluctance motor prototype [39]. The rated speed was about 3000 rpm. HTS YBCO bulks were used as the magnetic resistance medium of the rotor quadrature axis, thus the output torque, power density and efficiency were much improved.

B. HTS Maglev

The Southwest Jiaotong University (SWJTU) has initiated the HTS maglev vehicle research since 1994. The people-carrying HTS maglev vehicle was tested successfully at the end of 2000 [40]. There were 8 HTS maglev modules in the vehicle body. Each module consisted of 43 YBCO bulks in a liquid nitrogen vessel. The YBCO bulks were 30 mm in diameter and 17–18 mm in thickness. An update HTS maglev measurement system was developed in 2004 to verify the design of an iron flux-collector and Halbach PM array. A renewed HTS maglev dynamic test system was developed for the experimental tests at a velocity from 0 to 300 km/h.

C. HTS Linear Machines

The UESTC group has developed a 1-kN levitated single-sided HTS linear synchronous motor (HTSLSM) commencing in 2007 [41]. The primary and secondary were composed of copper windings with tooth-slot structure and an YBCO bulk magnet array. The magnet array consisted of 30 rectangular YBCO bulk magnets, which were installed in a cryogenic vessel to form 6 magnetic poles with alternate polarities along the moving direction and 5 identical poles installed side by side along the transversal direction. 70 cylindrical YBCO bulks were used in the HTS magnetic suspension subsystem, in which two types of permanent magnetic guideways were developed with surface-mounted and flux concentrated permanent magnets.

Further development on the above model, was carried out by the UESTC group which has also invented two different HTS linear synchronous generators for power generation using renewable energy from the tide and from solar, in which both HTS bulks and HTS coils are implanted in their secondary movers [42], [43].

IV. HTS Magnets and Applications

A. HTS Magnetic Separator

HTS has demonstrated advantages for building a high gradient magnetic separator [44]. The IEE CAS developed a HTS magnetic separator for the potential use in the waste-water treatments [45]. The separator system had a diameter of 46 mm, a height of 240 mm, and had an effective volume of 0.398 L. The separator system consisted of steel wire to generate high magnetic field gradient, with the weight of about 76 g, the size of $\Phi 60\ \mu\text{m} \times 30$ mm, and void factor of 2.1%. The HTS magnet was 202.8 mm in length and 120 mm in inner diameter. The central operating magnetic field was a nominal 3.2 T with an operating current of 120 A. The HTS magnet wound by BSCCO 2223 tapes was cooled by a two-stage GM cryocooler at 20 K. The current lead of the HTS magnet system was designed as a hybrid structure including a copper section, a BSCCO 2223 bulk lead section and a section made by BSCCO 2223 Ag tapes. The current lead was designed to operate with the warm end at about 40–50 K and the cold end at 20 K.

B. Split Superconducting Magnet

The IEE CAS developed a superconducting magnet system with a large crossing warm bore for the national high magnetic field laboratory [46]. It consisted of 8 coaxial coils and was assembled in the form of split coil groups. Both HTS BSCCO 2223 tape and LTS NbTi wires were used to generate the central magnetic field of 8 T. The outer NbTi coils provided the background field of 5.3 T, and the inner BSCCO 2223 coils contributed the additional 2.7 T to the central field. The whole magnet system was cooled with two GM cryocoolers. The separation gap of the split coils was set at 136 mm to facilitate the installation of a crossing warm bore.

C. HTS Magnet for Propulsion Experiment

The IEE CAS developed a HTS magnet system for the propulsion experiment [47]. It consisted of two split HTS coils, a cryostat, a cryocooler, and a coaxial piston coil with a shaft. The HTS magnet wound by BSCCO 2223 tapes was split into two parts, with each half composed of 6 pancake coils. The split pair magnet was used to produce a radial magnetic field distribution inside the clear bore for the piston coil propulsion. The magnet produced a maximum radial magnetic field of 0.55 T in the clear bore when an operating current of 200 A was applied. When the piston coil was charged by a current of 3 A, it underwent a maximum axial force of 359 N within an axial displacement of 10 cm. The axial force drove the 2.59-kg piston coil with a maximum power output of 2182 W.

D. HTS Magnet with Solid Nitrogen Protection

The IEE CAS developed a conduction-cooled HTS magnet system with solid nitrogen protection. The HTS magnet system was used to investigate fast discharging performances with a constant output voltage [48]. The HTS magnet wound by BSCCO 2223 consisted of 14 double pancakes. Cryostat for the HTS magnet system was designed to cool the coils with a GM cryocooler together with the solid nitrogen protection technology. To acquire experiences of stand-alone operation of the HTS magnet system, the solid nitrogen was used to keep the magnet temperature constant for 40 hours after the cryocooler was shut down.

E. HTS Magnet in ExCES

The IEE CAS developed ultra-high magnetic field superconducting magnets and a center field of 25–30 T for the extreme condition of experimental science facility (ExCES). HTS YBCO and BSCCO 2223 inserts were fabricated and tested at 4.2 K to prove the technical feasibility to achieve the target of 25 T [49]. The BSCCO 2223 insert has the inner diameter, outer diameter, and height of 120 mm, 214 mm, and 250 mm, respectively. The YBCO insert has the inner diameter, outer diameter, and height of 22 mm, 65 mm, and 204 mm, respectively. The central operating magnetic field of the BSCCO 2223 insert can reach up to 5.8 T, while a 5.3-T central magnetic field can be obtained in the central bore of YBCO insert with the operation current of 150 A.

F. Superconducting Magnet in MRI

The Alltech Medical Systems in Chengdu, China, developed a 1.5-T superconducting magnet specially for a magnetic resonance imaging (MRI) system in 2009 [50]. The Alltech magnet has a relatively high uniformity, which makes the bare uniformity varying from 300–600 ppm on a 50-cm design spherical volume (DSV). On-site shimming for most of the systems can be finished within half a day with $+/-6$ ppm compared with before day's shimming. Recently over a hundred MRI systems have been delivered to customs. The 1.5-T MRI system and its scanned image are shown in Fig. 8. After the development and commercialization of the 1.5-T MRI system, the Alltech has worked with Academia and other medical institutions to provide multimodality products for health care. Besides MRI series products with 3-T and 7-T high-field MRI systems, Positron emission tomography integrated with MRI (PET/MRI) and minimally Invasive MR Guided Surgery, are under development—enabling patient centered treatment planning and delivery. To date, the Alltech MRI product uses NbTi wires, meanwhile the investigation of potential use of MgB_2 and HTS wires is being carried out.

G. HTS High-Q Power Resonator and Applications

By using a HTS inductor, a resonant circuit can achieve a very high Q value, consequently, special aspects such as a very high voltage can be built up much higher than using conventional technology or a very high current can be controlled for various applications, such as magnet or SMES charging, inductive heating, high-power wireless energy transferring, and high-voltage insulation testing. A high efficient wireless power transfer method using HTS coils has been developed for a novel concept of car charging without the need of stopping at a charging station and its patent has been granted. The HTS resonation method and practical devices have been verified by using a BSCCO 2223 inductor with a practical 1-kV device built in the UESTC [51].

Fig. 8. 1.5-T MRI product and its scanned image.

H. HTS Magnet Cannonball

By using a HTS bulk or a set of HTS bulks, a military cannon has been designed. The shell of the cannon has a super thrust due to the HTS strong magnetic reaction to an applied high field. Consequently a longer projectile distance and more powerful hit can be achieved. A patent has been granted to the UESTC for the innovation, which means a potential future war could be more green and environment friendly.

I. HTS Current Lead

The Institute of Plasma Physics, Chinese Academy of Sciences (ASIPP) developed a 68-kA BSCCO 2223 HTS current lead [52] for the international thermonuclear experimental reactor (ITER) and applied 13 pairs of 16-kA HTS current leads for the experimental advanced superconducting Tokamak (EAST), which can save 2/3 of refrigeration power consumption and reduce cooling equipment substantially compared with conventional copper current leads.

Now the HTS current leads, rated current less than 0.5 kA, are widely used for small- and mid-scale LTS magnets for magnetic separators, high-power microwave emitting, crystal growing and SMES; and for HTS magnets in ship motors and SMES. Based on the main heat source minimized by the HTS current leads the heat loads of these magnets are reduced by one or two orders of magnitude and consequently can be cooled with one or two GM cryocoolers and reach cryogen vaporizing-free or conduction cooling.

J. HTS Cooling Techniques

Cryo-cooling systems for HTS power applications are indispensible. There are several options for the demonstration applications in China: i) Multi-GM or Stirling cryocoolers plus a circulator pump are used for the LN_2-cooled HTS cables. ii) Two-stage Stirling or GM cryocoolers are employed for LNe cooled HTS motor and SMES magnets. iii) HTS FCLs and transformers are cooled with LN_2 supplied by air separation industries. The Stirling cryocoolers have higher efficiency, but short maintenance period less than 7000 hrs. The GM cryocoolers are more reliable in operation, but have a lower efficiency. The open cooling systems for FCLs and transformers without cryocoolers have the lowest cost.

V. Measurement and Characterization on HTS Applicable Properties

A. Measurements on Critical Currents

To realize the variable orientation of dc magnetic field in the standard four-probe method, an active technique is used by rotating the HTS sample in the static background of a dc magnetic field. The dc background magnet has the excitation coil and double E-type iron core with air gap and the HTS sample which is fixed on a holder can be rotated from 0° to 360°.

Although there are various contact-free measurement methods of critical currents [53], [54], the trapped field method and the magnetic-circuit method are readily implemented.

The magnetic-circuit method uses two magnetic circuits, exciting magnetic circuit and detecting magnetic circuit, to excite and measure HTS tapes, respectively. The specimen was transferred through the sample gap where the induced current drives the magnetic flux flowing through the detecting magnetic circuit, and the magnetic flux density was measured by a Hall sensor [55]. Its experimental resolution was smaller than 2 mm with a speed of 360 m/h.

B. Measurement on Mechanical Properties

In the set-up for measuring the stress/strain, a HTS sample was installed between two FGRP plates. The hydraulic-servo tensile machine provided the tensile force. A HTS sample was fixed at both ends to the gripping holders. The sample was continuously pulled up to irreversible stress/strain. The load and strain could be measured accurately by the motor control and transducers as well as the strain gauge [56] with sensitivity of 0.1 MPa.

C. Measurement on ac Losses

A calorimetric method by using optical fiber Bragg grating (FBG) was introduced [57]. Optical FBG is a sensor with a thin diameter and able to measure micro-strain which only results from temperature change due to ac loses in this test arrangement. This calorimetric method with resolution of 10^{-4} W/m is available for measuring the ac losses of superconductors and expected to be generalized to ac loss measurements in sophisticated electromagnetic environment.

D. Other Measurement Techniques

Measuring techniques developed for practical HTS applications also included: i) trapped field attenuation of HTS bulk magnet exposed to external traveling-wave magnetic field [58]; ii) noninductive HTS tape coil measurement for long wire ac loss and also for the HTS wire-type resistive FCLs [59]; iii) multifunctional HTS measurement and HTS device control platforms [60]–[63].

VI. Progress of Applied Superconductors

A. Progress of 1G HTS Tapes

The first production line of 1G HTS BSCCO 2223 tapes was set up in 2001 with an annual production capacity of 200 km at the InnoST. In 2003, the production capacity was up to 300 km [64]. During the past years, R&D efforts have been continuing to improve the application properties of the HTS tapes, such as reducing ac losses and thermal conductivity and increasing insulating properties. The latest products include normalized-type, insulated-type, reinforced-type and low-thermal-conductivity type BSCCO 2223 tapes. They were with the critical current I_c of 120–140 A and critical current density J_c of 12–14 kA/cm^2 at 77 K and self field. The BSCCO 2223 products from the InnoST have been successfully used and demonstrated in the ac and dc power cables, SFCLs, motors, transformer and maglev applications. Another BSCCO 2223 tape production line was built in 2003 in the Northwest Institute for Non-ferrous Metal Research (NIN) with the annual production capacity of 200 km.

B. Progress of 2G HTS Tapes

There are several groups in China working on the 2G tape production, including Shanghai University (SU), Shanghai Jiao Tong University (SJTU), Tsinghua University (TU), Beijing University of Technology (BUT), Beijing General Research Institute for Nonferrous Metals (BGRINM), NIN, Southwest Jiaotong University (SJU), Xi'an University of Technology (XUT), and Jilin University (JU), Institute of Solid State Physics, Chinese Academy of Sciences (ISSP CAS), IEE CAS, UESTC, and so on, as summarized in Table V [65]–[79]. They prepared the coated conductors for both buffer layers and superconducting layers by using physical vapour deposition techniques of sputtering or pulse laser deposition (PLD), as well as using the metallorganic chemical vapor or solution depositions (MOCVD, MOD). Some of them have established the reel-to-reel tools for scaling up of long tapes.

Very recently, Shanghai University has developed a creative way, a nonvacuum electrodeposition technique to prepare oxide buffer layers with excellent texture and morphology quality [69]. To combine the electrodeposition technique for buffer layers and extremely low-fluorine chemical solution for YBCO superconducting layers, allowing one to see promising cost-effective, and high-rate technical routes for the industrialization of YBCO coated conductors. A series of reel-to-reel home-made tools for scaling up manufacture of coated conductors in km level have been built in China such as the pilot line at the Shanghai Creative Superconductor Technologies Co., Ltd., as shown in Fig. 9.

C. Progress of Other Superconducting Materials

1) The NIN group initiated investigation on MgB_2 powder, wire, bulk and magnets in 2001 [80], and prepared the

TABLE V
MAIN RESEARCH GROUPS AND THEIR TECHNOLOGY ROUTES

Research Groups	Buffer Layer via		Superconducting Layer via		
	RABiTS	IBAD	MOCVD	PLD	MOD
TU	√	√			√
BUT	√				√
XUT					√
BGRINM	√R2R			√R2R	
NINM	√				
SJU	√				√
JU			√		
ISSP CAS	√				√
IEE CAS					√
SJTU	√R2R			√R2R	
SU	√R2R	√R2R		√	√R2R
UESTC	√R2R	√	√		

Fig. 9. Reel-to-reel production line for MOD-YBCO coating.

first 100-m level MgB_2 wire, and also developed the first MgB_2 magnet in China. The central magnetic field is about 2 T at 4.2 K. A km-level MgB_2 wire trial product was reported having engineering critical current density $J_e = 2.5 \times 10^4$ A/cm^2 at 20 K and 1 T [81]. Recently, the Southeast University has been devoted into the preparation of km-level MgB_2 wire. The proposed J_e and I_e are above 1×10^5 A/cm^2 and 100 A at 20-K and 2-T background field; and investigation to enhance the critical current of the MgB_2 wire has also been carried out [82]. The Southwest Jiaotong University has reported the cooperative doping effects of Ti and nano-SiC on the enhancement of in-field J_c performance of SiC doped MgB_2 tapes by a factor of 50-100% at 4.2 K and 10 T [83]. A series of HgO-doped MgB_2 samples have also been prepared and verified to achieve effective improvement of flux pinning together with very high impurity tolerance, which might provide another potential route to prepare high-performance MgB_2 bulks and wires on an industrial scale [84].

2) The layered rare-earth metal oxypnictides LnOFeAs (where Ln is La-Nd, Sm and Gd) are now attracting attention following the discovery of superconductivity at 26 K in the iron-based $LaO_{1-x}F_xFeAs$. The University of Science and Technology of China (USTC) reported discovery of bulk superconductivity in the related compound $SmFeAsO_{1-x}F_x$ in 2008 [85]. By replacing the La atoms with other rare-earth elements and modulating the structural parameters, T_c was enhanced in $CeFeAsO_{1-x}F_x$, $PrFeAsO_{1-x}F_x$, and $NdFeAsO_{1-x}F_x$ to above 50 K, doubling of the highest onset T_c of the 1111-type superconductors up to 55–57 K as reported by the Institute of Physics and Beijing National Laboratory for Condensed Matter Physics, Chinese Academy of Sciences (CAS) [86].

3) BGRINM fabricated HTS bulks from the very early HTS stage and applied the top-seeded melt-textured growth (TS-MTG) method for $YBa_2Cu_3O_{7-\delta}$ bulk preparations [87], [88]. Samples having the common size of 30 mm in diameter and 10 mm in thickness had a 15-N/cm^2 levitation force at 77 K and can be produced in batch quantity. The NIN group has also fabricated the $YBa_2Cu_3O_{7-\delta}$ bulks, CeO_2 addition for reducing the size of Y-211 particles and lower per-sintering temperature were studied and the sample's obtained maximum levitation force of 12.7 N/cm^2 [89]. Then multiseeds along c-axis powder melting process (MSPMP) to obtain a single domain $YBa_2Cu_3O_{7-\delta}$ bulk was explored [90].

Fig. 10. Large-area HTS film production line.

VII. HTS ELECTRONICS AND APPLICATIONS

A. Fabrication of HTS Thin Films

The developments of HTS thin film in China can be backdated to as early as 1987. Scientists in the Institute of Physics, Chinese Academy of Sciences (IOP CAS) reported their success in fabrication of YBCO thin films with zero resistance above 90 K [91], which is one of the earliest reports. After that, various advanced techniques including pulsed laser deposition, sputtering, co-evaporation, and "biaxial rotation" have been developed. A commercial company, named as the Tianjin Hi-tech Superconducting Electronics Co., Ltd., emerged in 2002. By using the co-evaporation technical route, as shown in Fig. 10, the company has realized DyBCO HTS films on a variety of substrate materials [92]. The chemical deposition techniques were also developed for potential industrial production, such as the photo-assisted MOCVD from the Jilin University [93] and the sol gel method from the Beihang University [94].

Apart from the 123 family ($YBa_2Cu_3O_{7-\delta}$, $DyBa_2Cu_3O_{7-\delta}$ etc.), Tl-2212 ($Tl_2Ba_2CaCu_2O_8$) film is another kind of important material from which excellent practical HTS filters can be fabricated. Scientists from the Nankai University have

been devoted to the research of Thallium thin film for almost two decades. Based on the success in Tl-2212 films, a series of S-band HTS filters have been developed. Some filters were being applied in the deep space detection network in China [95].

B. Design of HTS Filters

In the past decade, hundreds of HTS filters have been designed in China with central frequencies from 40 MHz [96] to up to 23 GHz [97]. Excellent performance with typical specifications such as 0.05 dB minimum insertion loss, 23 dB return loss [98], 110 dB out-of-band rejection [99] and 220 dB/MHz band-edge slope [100] etc. have been achieved. A smallest in volume ($\Phi 120$ mm $\times$ 175 mm) and weight (3.3 kg) HTS front-end subsystem was also constructed [101]. Some recent novel design methods and systems are described as follows: i) The IOP CAS group developed a new method for extracting a coupling matrix between the resonators from the simulated response curves in the design of resonator-based devices [102]. ii) For bandpass filters with wide stop band, the Tsinghua University group fabricated a compact HTS filter operating at 360 MHz by using modified spiral resonators with a tight three-turn spiral and inner/outer tails [103], a compact narrow-band six-pole HTS filter at the UHF-band using novel resonators with modified interdigital fingers and vertical meander lines [104], and a novel HTS band-pass filter with a very wide stopband using the method of staggered resonant modes [105]. iii) For the linear-phase filters, the UESTC group has developed a series of HTS linear-phase filters, including extracted-pole structure [106], parallel structure [107] and crossing line structure [108]. The UESTC group showed that with single-pole HTS group delay equalizer, the nonlinearity of phase variation of the filter by using external equalization linear-phase technique can be conveniently compensated and a flatter group delay can then be easily achieved [109], [110]. Tianjin Hi-tech also reported a high-performance linear-phase HTS filter, which has a center frequency of 830 MHz with 12-poles and 2 cross couplings, for 3G mobile communication [111]. iv) For the multiplexers, the Nankai University group developed a compact C-band HTS duplexer [112]. The Tsinghua University group reported the design method of microstrip contiguous diplexer at S-band with strong channel interaction [113] and designed a HTS microstrip quadruplexer at S-band with narrow channel bandwidth and spacing [114]. v) For the multiband and multimode filters, the Tianjin Hi-tech developed a dual-band HTS filter with 14-pole and 3 cross couplings on 2 inches MgO wafer. Cascaded quadruplet (CQ) coupling structures are employed to generate the proposed dual band filter. Each pair of zeros in CQ introduced by cross coupling can be tuned independently [115]. The research group in the East China of Jiaotong University, proposed a T-shaped stub-loaded split ring resonator (SRR) [116], a dual-band HTS bandpass filter by using a modified SRR [117] and two kinds of miniaturized HTS multimode bandpass filters [118], [119]. vi) For the tunable filters, the IOP CAS group constructed a 4-pole narrow-band bandpass filter employing semiconductor varactors [120]. The Tsinghua University group reported a tunable HTS resonator consisting of a microstrip spiral and a switchable interdigital capacitor array, controlled by low-loss mechanical switches [121], and a L-band HTS continuously tunable bandpass filter with dual-mode resonator and Gallium arsenide (GaAs) varactors [122].

C. Applications of HTS Filters

The most attractive application of HTS filters is in the base station of mobile communications. The Tsinghua University group has designed and fabricated a 14-pole HTS bandpass filter for code-division multiple access (CDMA) communication systems [123]. The HTS filter subsystem is installed in a CDMA base station in urban area of Tianjin as first field trial of the HTS filter subsystem on a single CDMA base station (BTS) [124]. Thereafter, a demonstration wireless communication cluster with HTS filter subsystems was built in the urban area of Beijing [125]. The Tianjin Hi-tech also conducted HTS subsystem field trial in CDMA base stations in Tianjin from 2004. Based on the success of constructing a HTS filter being able to handle up to 11.7-W power [126], the IOP CAS group constructed the world first HTS transceiver which works in the same frequency band to meet one of the 3G mobile communication standards, i.e., time-division-synchronous code multiple access (TD-SCDMA) [127].

Another interesting application of HTS filters is in Radar systems, e.g., the wind-profile radar. The IOP CAS group introduced a HTS front-end to meteorological radar for the first time, constituting the so-called HTS wind profiler [128]–[130]. Laboratory tests proved that, with HTS subsystem, improvements of sensitivity (3.8 dB) and interference rejection (48.4 dB) have been achieved [129].

Applications in radio astronomy are also interesting. The first HTS wideband filter for radio astronomy observation was made by IOP CAS group for space science research [98], [131]. HTS filters constructed by the China Electronics Technology Corporation (No. 16 Institute of CETC) were deployed in the deep space stations of Chinese lunar exploration project, which played an important role in monitoring the mission of Chang'e No. 3 satellite. More HTS filters are required for the construction of the deep space monitoring network in China.

As for the applications in space technology, the first ground test system in China showed that a reduction of 73% in noise temperature was obtained by substituting the HTS front-end for its conventional counterpart and passed all the space qualification tests in 2005 [132]. The space experimental system for HTS filter was then constructed by the IOP CAS and the Lanzhou Institute of Physics, China Aerospace Science and Technology Corporation (LZIP CASC). On October 14, 2012 the HTS experimental system was successfully launched into orbit by the Long March Rocket as a payload of a civil experimental satellite for new technologies, as shown in Fig. 11. On orbit experimental data received showed that the HTS system worked perfectly for the past 18 months. This is the world second success in space experiment for HTS devices after the high-temperature superconductivity space experimental (HTSSE) program. Application of the HTS filter front-end in a followed space science project is also being carried out [133].

VIII. Conclusion

Applied HTS technologies including materials, devices, cryogenics, measurements and automations have been practically developed to suit applicable devices in a broad range as

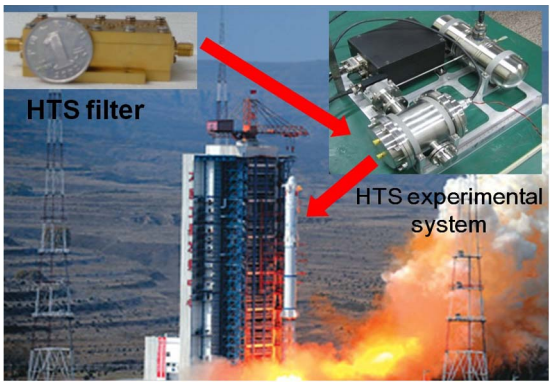

Fig. 11. First HTS space experiment for HTS filter in China.

described and analyzed, covering electrical and electronic, i.e., large and small, or strong and weak current applications. The detailed specifications extracted from the first HTS application approaches verify the applied HTS technologies to be further enabled for the next stage of HTS practical applications systematically, and the analysis has the relevant HTS technologies weighted to be industrialized. The research outcomes, project status, and device performance details presented reveal the trend and distance to reach the goal of industrial applications of the applied HTS materials and technologies.

ACKNOWLEDGMENT

The authors would thank J. Du, S. X. Dou, Y. F. Bi, X. Y. Chen, Y. D. Jiang, L. Sun, J. S. Cheng, C. Gu, R. M. Sun, C. L. Tang, T. Coombs, R. H. Qu, W. Xu, Y. G. Guo, J. G. Zhu, C. Grantham, F. Rahman, G. X. Wang, and C. Sorrell for the assistance to the work.

REFERENCES

[1] Y. Xin *et al.*, "Development of saturated iron core HTS fault current limiters," *IEEE Trans. Appl. Supercond.*, vol. 17, no. 2, pp. 1760–1763, Jun. 2007.
[2] Y. Xin *et al.*, "Saturated iron-core superconductive fault current limiter developed at Innopower," in *Proc. AIP Conf.*, 2014, vol. 1573, pp. 1042–1048.
[3] J. B. Cui *et al.*, "Safety considerations in the design, fabrication, testing, and operation of the dc bias coil of a saturated iron-core superconducting fault current limiter," *IEEE Trans. Appl. Supercond*, vol. 23, no. 3, p. 5600704, Jun. 2013.
[4] W. Z. Gong *et al.*, "HTS dc bias coil for 35-kV/90 MVA saturated iron-core fault current limiter," *Phys. C, Supercond.*, vol. 468, no. 15–20, pp. 2050–2053, Sep. 2008.
[5] Y. Xin *et al.*, "Manufacturing and test of a 35-kV/90 MVA saturated iron-core type superconductive fault current limiter for live-grid operation," *IEEE Trans. Appl. Supercond.*, vol. 19, no. 3, pp. 1934–1937, Jun. 2009.
[6] Y. Xin *et al.*, "Performance of the 35-kV/90 MVA SFCL in live-grid fault current limiting tests," *IEEE Trans. Appl. Supercond.*, vol. 21, no. 3, pp. 1294–1297, Jun. 2011.
[7] Y. W. Sun *et al.*, "DC bias system of a 35-kV/90 MVA saturated iron core SFCL," *Cryogenics*, vol. 51, no. 6, pp. 257–260, Jun. 2011.
[8] Y. Xin *et al.*, "Development of a 220-kV/300 MVA superconductive fault current limiter," *Supercond. Sci. Technol.*, vol. 25, no. 10, p. 105011, Oct. 2012.
[9] Y. Xin *et al.*, "Factory and field tests of a 220-kV/300 MVA statured iron-core superconducting fault current limiter," *IEEE Trans. Appl. Supercond.*, vol. 23, no. 3, p. 5602305, Jun. 2013.
[10] D. Hui *et al.*, "Development and test of 10.5-kV/1.5 kA HTS fault current limiter," *IEEE Trans. Appl. Supercond.*, vol. 16, no. 2, pp. 687–690, Jun. 2006.
[11] Z. Hong, J. Sheng, L. Yao, J. Gu, and Z. Jin, "The structure, performance and recovery time of a 10-kV resistive type superconducting fault current limiter," *IEEE Trans. Appl. Supercond.*, vol. 23, no. 3, p. 5601304, Jun. 2013.
[12] Y. Guo, L. Y. Xiao, and S. T. Dai, "Enhancing low-voltage ride-through capability and smoothing output power of DFIG with a superconducting fault-current limiter–magnetic energy storage system," *IEEE Trans. Energy Convers.*, vol. 27, no. 2, pp. 277–295, Jun. 2012.
[13] J. X. Jin *et al.*, "Electrical application of high T_c superconducting saturable magnetic core fault current limiter," *IEEE Trans. Appl. Supercond.*, vol. 7, no. 2, pp. 1009–1012, Jun. 1997.
[14] J. X. Jin, S. X. Dou, H. K. Liu, and C. Grantham, "Preparation of high T_c superconducting coils for consideration of their use in a prototype fault current limiter," *IEEE Trans. Appl. Supercond.*, vol. 5, no. 2, pp. 1054–1051, Jun. 1995.
[15] J. X. Jin, X. K. Fu, H. K. Liu, and S. X. Dou, "Performance and applications of bulk Bi-2223 HTS bars produced using a hot-press technique," *Phys. C, Supercond.*, vol. 341–348, no. 1–4, pp. 2621–2622, Nov. 2000.
[16] L. Jiang, J. X. Jin, and X. Y. Chen, "A full controlled hybrid bridge type superconducting fault current limiter," *IEEE Trans. Appl. Supercond.*, vol. 24, no. 5, 2014, DOI: 10.1109/TASC.2014.2351264.
[17] Y. Xin *et al.*, "China's 30 m, 35-kV/2 kA ac HTS power cable project," *Supercond. Sci. Technol.*, vol. 17, no. 5, pp. 332–336, May 2004.
[18] Y. Xin *et al.*, "Introduction of China's first live grid installed HTS power cable system," *IEEE Trans. Appl. Supercond.*, vol. 15, no. 2, pp. 1841–1847, Jun. 2005.
[19] L. Y. Xiao *et al.*, "Development of HTS AC power transmission cables," *IEEE Trans. Appl. Supercond.*, vol. 17, no. 2, pp. 1652–1655, Jun. 2007.
[20] S. T. Dai *et al.*, "Testing and demonstration of a 10-kA HTS DC power cable," *IEEE Trans. Appl. Supercond.*, vol. 24, no. 2, p. 5400104, Apr. 2014.
[21] Q. Huang, J. X. Jin, and J. B. Zhang, "Simulation study on performance of a long-distance superconducting DC power transmission system," *Elect. Power*, vol. 39, no. 3, pp. 45–49, 2006.
[22] J. X. Jin, "High efficient DC power transmission using high-temperature superconductors," *Phys. C, Supercond.*, vol. 460–462, pp. 1443–1444, Sep. 2007.
[23] Q. L. Wang *et al.*, "Design and fabrication of a conduction-cooled high temperature superconducting magnet for 10 kJ superconducting magnetic energy storage system," *IEEE Trans. Appl. Supercond.*, vol. 16, no. 2, pp. 570–573, Jun. 2006.
[24] Q. L. Wang *et al.*, "A 30 kJ Bi2223 high temperature superconducting magnet for SMES with solid-nitrogen protection," *IEEE Trans. Appl. Supercond.*, vol. 18, no. 2, pp. 754–757, Jun. 2008.
[25] S. T. Dai *et al.*, "Design of a 1 MJ/0.5 MVA HTS magnet for SMES," *IEEE Trans. Appl. Supercond.*, vol. 17, no. 2, pp. 1977–1980, Jun. 2007.
[26] Q. L. Wang *et al.*, "Development of large scale superconducting magnet with very small stray magnetic field for 2 MJ SMES," *IEEE Trans. Appl. Supercond.*, vol. 20, no. 3, pp. 1352–1355, Jun. 2010.
[27] J. Shi *et al.*, "Development of a conduction-cooled HTS SMES," *IEEE Trans. Appl. Supercond.*, vol. 17, no. 3, pp. 3846–3852, Sep. 2007.
[28] X. H. Jiang, X. G. Zhu, Z. Cheng, X. Ren, and Y. He, "A 150-kVA/0.3 MJ SMES voltage sag compensation system," *IEEE Trans. Appl. Supercond.*, vol. 15, no. 2, pp. 1903–1906, Jun. 2005.
[29] J. H. Zhu *et al.*, "Experimental research on dynamic voltage sag compensation using 2G HTS SMES," *IEEE Trans. Appl. Supercond.*, vol. 21, no. 3, pp. 2126–2130, Jun. 2011.
[30] J. Y. Zhang *et al.*, "Electric energy exchange and applications of superconducting magnet in an SMES device," *IEEE Trans. Appl. Supercond.*, vol. 24, no. 3, p. 5700704, Jun. 2014.
[31] Y. S. Wang *et al.*, "Development of solenoid and double pancake windings for a three-phase 26-kVA HTS transformer," *IEEE Trans. Appl. Supercond.*, vol. 14, no. 2, pp. 924–927, Jun. 2004.
[32] Y. S. Wang *et al.*, "Development of a 45-kVA single-phase model HTS transformer," *IEEE Trans. Appl. Supercond.*, vol. 16, no. 2, pp. 1477–1480, Jun. 2006.
[33] Y. S. Wang *et al.*, "Development of a 630-kVA three-phase HTS transformer with amorphous alloy cores," *IEEE Trans. Appl. Supercond.*, vol. 17, no. 2, pp. 2051–2054, Jun. 2007.
[34] X. S. Li, Q. F. Chen, J. Sun, Y. Zhang, and G. Long, "Analysis of magnetic field and circulating current for HTS transformer windings," *IEEE Trans. Appl. Supercond.*, vol. 15, no. 3, pp. 3808–3813, Sep. 2005.
[35] Y. D. Jiang, "HTS wind turbine project in DEC," in *Proc. Int. Workshop Elect. Mach. HTS Technol. Wind Power Appl.*, Chengdu, China, May 29–31, 2013.

[36] Y. D. Jiang *et al.*, "Development of a 400 m YBCO racetrack coil for HTS machine applications," in *Proc. IEEE Int. Conf. Appl. Supercond. Electromagn. Devices*, Beijing, China, Oct. 25–27, 2013, pp. 500–503.

[37] Z. Zhu, R. H. Qu, and J. Wang, "Conceptual design of the cryogenic system for a 12 MW superconducting wind turbine generator," *IEEE Trans. Appl. Supercond.*, vol. 24, no. 3, p. 520115, Jun. 2014.

[38] J. Zheng *et al.*, "The study and test for 1MW high temperature superconducting motor," *IEEE/CSC ESAS Eur. Supercond. News Forum*, no. 2, pp. 1–4, Oct./Nov. 2012.

[39] M. Qiu *et al.*, "Design and performance of a small HTS bulk reluctance motor," *IEEE Trans. Appl. Supercond.*, vol. 15, no. 2, pp. 1480–1483, Jun. 2005.

[40] J. S. Wang *et al.*, "The first man-loading high temperature superconducting Maglev test vehicle in the world," *Phys. C, Supercond.*, vol. 378–381, pp. 808–814, Oct. 2002.

[41] Z. H. Wu and J. X. Jin, "Characteristic analysis of HTS linear synchronous generators designed with HTS bulks and tapes," *IEEE Trans. Appl. Supercond.*, vol. 24, no. 5, p. 5202805, Oct. 2014.

[42] Z. H. Wu and J. X. Jin, "Novel concept of dish Stirling solar power generation designed with an HTS linear generator," *IEEE Trans. Appl. Supercond.*, vol. 24, no. 5, 2014, DOI: 10.1109/TASC.2014.2351257.

[43] J. X. Jin *et al.*, "High-temperature superconducting linear synchronous motors integrated with HTS magnetic levitation components," *IEEE Trans. Appl. Supercond.*, vol. 22, no. 5, p. 5202617, Oct. 2012.

[44] J. X. Jin *et al.*, "A high gradient magnetic separator fabricated using Bi-2223/Ag HTS tapes," *IEEE Trans. Appl. Supercond.*, vol. 9, no. 2, pp. 394–397, Jun. 1999.

[45] L. G. Yan, "Recent progress of superconducting magnet technology in China," *IEEE Trans. Appl. Supercond.*, vol. 20, no. 3, pp. 123–134, Jun. 2010.

[46] Y. M. Dai *et al.*, "An 8 T superconducting split magnet system with large crossing warm bore," *IEEE Trans. Appl. Supercond.*, vol. 20, no. 3, pp. 608–611, Jun. 2010.

[47] Q. L. Wang, *Practical Design of Magnetostatic Structure Using Numerical Simulation*. Singapore: Wiley, 2013.

[48] Y. M. Dai *et al.*, "High temperature superconducting magnet for fast discharging experiments," *IEEE Trans. Appl. Supercond.*, vol. 17, no. 2, pp. 2208–2211, Jun. 2007.

[49] Q. L. Wang *et al.*, "High magnetic field superconducting magnet system up to 25 T for ExCES," *IEEE Trans. Appl. Supercond.*, vol. 23, no. 3, p. 4300905, Jun. 2013.

[50] Z. M. Wang, "Superconducting magnet of magnetic resonance imaging system," in *Proc. IEEE Int. Conf. Appl. Supercond. Electromagn. Devices*, Beijing, China, Oct. 25–27, 2013, pp. 530–534.

[51] J. X. Jin, C. M. Zhang, Y. G. Guo, and J. G. Zhu, "Theory and operation principle of a HTS high Q resonant circuit," *IEEE Trans. Appl. Supercond.*, vol. 17, no. 2, pp. 2022–2025, Jun. 2007.

[52] P. Bauer *et al.*, "R&D towards HTS current leads for ITER," *IEEE Trans. Appl. Supercond.*, vol. 19, no. 3, pp. 1500–1503, Jun. 2009.

[53] J. H. Zhu, M. Qiu, and J. T. Tian, "A novel method on the critical current test of YBCO HTS tape," *Cryogenics Supercond.*, vol. 37, no. 5, pp. 16–19, 2009.

[54] Y. S. Wang *et al.*, "Detecting and describing the homogeneity of critical current in practical long HTS tapes using contact-free method," *Cryogenics*, vol. 47, pp. 225–231, 2007.

[55] S. N. Zou, C. Gu, T. M. Qu, and Z. Han, "Continuous critical current measurement of high-temperature superconductor tapes with magnetic substrates using magnetic-circuit method," *Rev. Sci. Instru.*, vol. 84, no. 10, pp. 105106-1–105106-7, Oct. 2013.

[56] M. Qiu *et al.*, "Strain effect of YBCO coated conductor on transport characteristics," *Supercond. Sci. Technol.*, vol. 20, no. 3, pp. 162–167, Mar. 2007.

[57] J. S. Dai, Y. S. Wang, W. J. Zhao, L. M. Xia, and D. Sun, "A novel calorimetric method for measurement of AC losses of HTS tapes by optical Fiber Bragg Grating," *IEEE Trans. Appl. Supercond.*, vol. 24, no. 5, p. 9002104, Oct. 2014.

[58] J. X. Jin, L. H. Zheng, W. Xu, Y. Guo, and J. Zhu, "Influence of external traveling-wave magnetic field on trapped field of a high temperature superconducting bulk magnet in a linear synchronous motor," *J. Appl. Phys.*, vol. 109, no. 11, pp. 113913-1–113913-4, Jun. 2011.

[59] J. X. Jin, S. X. Dou, T. Hardono, and C. Cook, "Novel AC loss measurement of high T_c superconducting long wire," *Phys. C, Supercond.*, vol. 314, no. 3/4, pp. 285–290, Mar. 1999.

[60] L. H. Zheng and J. X. Jin, "Measurement and device control using a computer-based platform," *Appl. Supercond. Electromagn.*, vol. 2, no. 1, pp. 72–80, 2011.

[61] L. Wen *et al.*, "A universal LabVIEW-based HTS device measurement and control platform and verified through a SMES system," *IEEE Trans. Appl. Supercond.*, vol. 24, no. 5, 2014, DOI: 10.1109/TASC.2014.2349897.

[62] L. Wen, Y. Chen, and J. X. Jin, "A compound control system for a PMLSM based on virtual instrument and digital signal processor," in *Proc. IEEE Int. Conf. Appl. Supercond. Electromagn. Devices*, Beijing, China, Oct. 25–27, 2013, pp. 504–507.

[63] L. Wen, X. Y. Chen, L. Jiang, and J.X. Jin, "LabVIEW-based intelligent platform for HTS measurements," in *Proc. IEEE Int. Conf. Appl. Supercond. Electromagn. Devices*, Beijing, China, Oct. 25–27, 2013, pp. 378–379.

[64] H. P. Yi *et al.*, "Research status of the manufacturing technology and application properties of Bi-2223/Ag tapes at Innost," *Phys. C, Supercond.*, vol. 412–414, pp. 1073–1078, Oct. 2004.

[65] L. L. Ying *et al.*, "Epitaxial growth of $La_2Zr_2O_7$ buffer layers for $YBa_2Cu_3O_{7-\delta}$ coated conductors on metallic substrates using pulsed laser deposition," *Phys. C, Supercond.*, vol. 469, no. 7/8, pp. 288–292, Apr. 2009.

[66] L. L. Ying *et al.*, "Hickness effect of $La_2Zr_2O_7$ single buffers on metallic substrates using pulsed laser deposition for $YBa_2Cu_3O_7$ coated conductors," *Supercond. Sci. Technol.*, vol. 22, no. 9, p. 095005, Sep. 2009.

[67] L. L. Ying *et al.*, "Deposition of $Gd_2Zr_2O_7$ single buffer layers with different thickness for $YBa_2Cu_3O_{7-\delta}$ coated conductors on metallic substrates," *Phys. C, Supercond.*, vol. 470, no. 13/14, pp. 543–546, Jul. 2010.

[68] F. Fan *et al.*, "Epitaxial growth of $Ce_2Y_2O_7$ buffer layers for $YBa_2Cu_3O_{7-\delta}$ coated conductors using reel-to-reel DC reactive sputtering," *Phys. C, Supercond.*, vol. 471, no. 15, pp. 471–475, Aug. 2011.

[69] L. N. Sang *et al.*, "Cost-effective electrodeposition of an oxide buffer for high-temperature superconductor coated conductors," *Supercond. Sci. Technol.*, vol. 27, no. 6, p. 065016, Jun. 2014.

[70] Q. Q. Zhang *et al.*, "Epitaxial growth of $YBa_2Cu_3O_7$ films on $SrTiO_3$ (100) by direct solution precursor deposition," *J. Phys., Conf. Ser.*, vol. 507, no. 1, p. 012055, 2014.

[71] W. Wu *et al.*, "A low-fluorine solution with a 2:1 F/Ba mole ratio for the fabrication of YBCO films," *Supercond. Sci. Technol.*, vol. 27, no. 5, p. 055006, Mar. 2014.

[72] Y. M. Lu *et al.*, "Epitaxial growth of $Gd_2Zr_2O_7/Y_2O_3$ buffer layers for $YBa_2Cu_3O_{7-\delta}$ coated conductors," *Phys. C, Supercond.*, vol. 485, pp. 15–19, Feb. 2013.

[73] R. Zhao *et al.*, "Effect of Y_2O_3 seed layer on epitaxial growth of oxide barrier layer for YBCO coated conductor," *IEEE Trans. Appl. Supercond.*, vol. 23, no. 3, p. 6602104, Jun. 2013.

[74] Y. Xu *et al.*, "An effective substrate surface decoration to YBCO films by multiphase nanoparticles," *Phys. C, Supercond.*, vol. 495, pp. 187–191, Dec. 2013.

[75] H. Zhang *et al.*, "Film thickness dependence of microstructure and superconductive property of PLD prepared YBCO layers," *Phys. C, Supercond.*, vol. 499, pp. 54–56, Apr. 2014.

[76] D. Xu, Y. Wang, L. Liu, and Y. Li, "Dependences of microstructure and critical current density on the thickness of $YBa_2Cu_3O_{7-x}$ film prepared by pulsed laser deposition on buffered Ni-W tape," *Thin Solid Films*, vol. 529, no. 10, pp. 10–14, Feb. 2013.

[77] F. Z. Ding *et al.*, "Enhanced flux pinning in MOD-YBCO films with co-doping of $BaCeO_3$ and Y_2O_3 nanoparitcles," *Acta Phys. Sin.*, vol. 62, no. 13, p. 137 401, Jul. 2013.

[78] Y. D. Xia *et al.*, "Reel-to-reel deposition of epitaxial double-sided Y_2O_3 buffer layers for coated conductors," *Phys. C, Supercond.*, vol. 476, pp. 48–53, Jun. 2012.

[79] W. Li *et al.*, "Fabrication of $GdBa_2Cu_3O_{7-\delta}$ films by photo-assisted-MOCVD process," *Phys. C, Supercond.*, vol. 501, pp. 1–6, Jun. 2014.

[80] Y. Feng *et al.*, "Superconducting properties of MgB_2 wires and tapes with different metal sheaths," *Phys. C, Supercond.*, vol. 386, pp. 598–602, Apr. 2003.

[81] C. S. Li *et al.*, "Fabrication and properties of kilometer level multifilamentary MgB_2/Nb/Cu wires," *Chin. J. Low Temp. Phys.*, vol. 34, no. 4, pp. 292–296, 2012.

[82] Z. X. Shi *et al.*, "Anisotropic connectivity and its influence on critical current densities, irreversibility fields, and flux creep in in-situ processed MgB_2 strands," *Supercond. Sci. Technol.*, vol. 23, no. 4, p. 045018, Apr. 2010.

[83] X. F. Pan, A. Matsumoto, H. Kumakura, C. H. Cheng, and Y. Zhao, "Cooperative doping effects of Ti and nano-SiC on transport critical current density and grain connectivity of in situ MgB_2 tapes," *Phys. C, Supercond.*, vol. 471, no. 21/22, pp. 1128–1132, Nov. 2011.

[84] Y. J. Cui *et al.*, "Significant enhancement of critical current density in MgB_2 with HgO doping under high pressure," *Phys. Stat. Sol. (A)*, vol. 207, no. 11, pp. 2532–2537, Nov. 2010.

[85] X. H. Chen *et al.*, "Superconductivity at 43 K in $SmFeAsO_{1-x}F_x$," *Nature*, vol. 453, no. 7196, pp. 761–762, Jun. 2008.

[86] Z. A. Ren and Z. X. Zhao, "Research and prospects of iron-based superconductors," *Adv. Mater.*, vol. 21, no. 45, pp. 4584–4592, Dec. 2009.

[87] H. T. Ren *et al.*, "Batch process of single domain YBCO bulk superconductors," *Chin. J. Low Temp. Phys.*, vol. 25, no. 1, pp. 11–16, 2003.

[88] Y. X. Chen *et al.*, "Effects of process parameters on YBCO bulks prepared by TSMTG," *J. Chin. Rare Earth Soc.*, vol. 21, no. 5, pp. 526–529, 2003.

[89] X. D. Tang *et al.*, "Effects of refinement of Y-211 particles and lower oxygenation temperature on the superconducting properties of bulk YBCO," *Chin. J. Low Temp. Phys.*, vol. 25, no. 1, pp. 202–206, 2003.

[90] C. P. Zhang *et al.*, "Insetting multi-seeds for YBCO single domain depth growth," *Chin. J. Low Temp. Phys.*, vol. 31, no. 4, pp. 301–305, 2009.

[91] B. R. Zhao *et al.*, "Superconductivity at 89K of Ba-Y-Cu-O thin films," *Chin. Phys. Lett.*, vol. 4, no. 6, pp. 280–283, Jun. 1987.

[92] T. B. Tao *et al.*, "Speed modulation technique to achieve simultaneous deposition of 3-in double-sided Y-Ba-Cu-O thin films," *Phys. C, Supercond.*, vol. 433, no. 1/2, pp. 87–92, Dec. 2005.

[93] W. Li, S. Li, G. Li, B. Zhang, and P. Chou, "Thickness dependence of structural and superconducting properties of single-crystal-like GdBCO films prepared by photo-assisted MOCVD," *IEEE Trans. Appl. Supercond.*, vol. 23, no. 2, p. 7200606, Jun. 2013.

[94] Y. S. He *et al.*, "Plenary talk—Developments of HTS microwave passive and active devices and their applications in space and on ground," in *Proc. IEEE Int. Conf. Appl. Supercond. Electromagn. Devices*, Beijing, China, Oct. 25-27, 2013, p. 267.

[95] H. Xia *et al.*, "Development of high-temperature superconducting filters operating at temperatures above 90 K," *Chin. Sci. Bull.*, vol. 54, no. 19, pp. 3596–3599, Oct. 2009.

[96] Y. Zhang *et al.*, "An ultracompact superconducting bandpass filter at 40 MHz using spiral resonators and a new feedline structure," *IEEE Trans. Appl. Supercond.*, vol. 22, no. 2, p. 1500205, Apr. 2012.

[97] J. Guo *et al.*, "A 12-pole K-band wideband high-temperature superconducting microstrip filter," *IEEE Trans. Appl. Supercond.*, vol. 22, no. 2, p. 1500106, Apr. 2012.

[98] T. Yu *et al.*, "A wideband superconducting filter using strong coupling resonators for radio astronomy observatory," *IEEE Trans. Microw. Theory Tech.*, vol. 57, no. 7, pp. 1783–1789, Jul. 2009.

[99] J. Chen *et al.*, "A compact integration of high-temperature superconducting bandpass and bandstop filters," *Int. J. Mod. Phys. B*, vol. 19, no. 1–3, pp. 387–389, Jan. 2005.

[100] S. Li *et al.*, "A 12-pole narrowband highly selective high-temperature superconducting filter for the application in the third-generation wireless communications," *IEEE Trans. Microw. Theory Tech.*, vol. 55, no. 4, pp. 754–759, Apr. 2007.

[101] Y. B. Bian *et al.*, "A miniaturized HTS microwave receiver front-end subsystem for radar and communication applications," *Phys. C, Supercond.*, vol. 470, no. 15/16, pp. 617–621, Aug. 2010.

[102] F. Li *et al.*, "A new coupling matrix extracting method from the frequency response," *IEEE Trans. Microw. Theory Tech.*, vol. 55, no. 4, pp. 760–767, Apr. 2007.

[103] Z. J. Ying, "A compact superconducting bandpass filter at 360 MHz with very wide stopband using modified spiral resonators," *IEEE Trans. Appl. Supercond.*, vol. 23, no. 1, p. 1500706, Feb. 2013.

[104] J. C. Wang, "A UHF-band narrow-band HTS bandpass filter with wide stopband using interdigital structure," *IEEE Trans. Appl. Supercond.*, vol. 23, no. 6, p. 1502108, Dec. 2013.

[105] J. C. Wang, "A wide stopband band-pass HTS filter with staggered resonators," *Phys. C, Supercond.*, vol. 495, pp. 79–83, Dec. 2013.

[106] T. L. Zhang *et al.*, "The design of open-loop resonator HTSC linear-phase filter," *Cryogenics*, vol. 47, no. 7/8, pp. 409–412, Jul./Aug. 2007.

[107] T. L. Zhang, K. Yang, Y. F. Zhang, H. Jin, and Z. X. Luo, "Parallel-coupled linear-phase superconducting filter," *Chin. Sci. Bull.*, vol. 59, no. 16, pp. 1925–1928, 2014.

[108] T. L. Zhang, K. Yang, G. S. Kong, and Z. X. Luo, "Miniature linear-phase superconducting filter with group delay equalization," *Chin. Sci. Bull.*, vol. 55, no. 15, pp. 1453–1458, May 2010.

[109] L. Sun *et al.*, "An HTS microstrip equalizer for improving the group delay of an HTS filter for third-generation communications," *Supercond. Sci. Technol.*, vol. 21, no. 3, p. 035003, Mar. 2008.

[110] T. Zhang, K. Yang, and Z. Luo, "Development of integration HTSC linear phase filter with external equalization," *IEEE Trans. Appl. Supercond.*, vol. 23, no. 4, p. 1501805, Aug. 2013.

[111] L. Ji *et al.*, "Design and performance of superconducting filter with a linear phase for CDMA2000 communication system," *Sci. Chin. Inf. Sci.*, vol. 53, no. 9, pp. 1903–1907, Sep. 2010.

[112] X. Zhang *et al.*, "Compact design of high-temperature superconducting duplexer and triplexer for satellite communications," *Supercond. Sci. Technol.*, vol. 25, no. 10, p. 105 005, Oct. 2012.

[113] Y. Heng, "Design and optimization of a superconducting contiguous diplexer comprising doubly terminated filters," *IEEE Trans. Appl. Supercond.*, vol. 23, no. 4, p. 1501706, Aug. 2013.

[114] Y. Heng, "A narrowband superconducting quadruplexer with high isolation," *IEEE Trans. Appl. Supercond.*, vol. 24, no. 2, p. 1500506, Apr. 2014.

[115] L. Ji *et al.*, "Design and performance of dual-band high temperature superconducting filter," *Sci. Chin. Inf. Sci.*, vol. 55, no. 4, pp. 956–961, Apr. 2012.

[116] H. W. Liu, Y. Wang, Y.-C. Fan, X.-H. Guan, and Y. He, "Triple-band high-temperature superconducting microstrip filter based on multimode split ring resonator," *Appl. Phys. Lett.*, vol. 103, no. 4, p. 142603, Sep. 2013.

[117] H. W. Liu *et al.*, "Dual-band superconducting bandpass filter using embedded split ring resonator," *IEEE Trans. Appl. Supercond.*, vol. 23, no. 3, p. 1300304, Jun. 2013.

[118] H. W. Liu *et al.*, "Compact high-temperature superconducting filter using multimode stub-loaded resonator," *IEEE Trans. Appl. Supercond.*, vol. 24, no. 2, p. 1500308, Apr. 2014.

[119] H. W. Liu *et al.*, "Compact dual-band superconducting bandpass filter using quadruple-mode resonator," *IEEE Trans. Appl. Supercond.*, vol. 24, no. 2, p. 4901204, Apr. 2014.

[120] N. Li *et al.*, "Low loss HTS tunable bandpass and bandstop filters in P-band," presented at the Applied Superconductivity Conference, Portland, OR, USA, 2012, Paper 12-A-156-ASC.

[121] Z. J. Ying, "Design and tuning of superconducting filter at VHF-band with mechanically switchable interdigital capacitors," *Electron. Lett.*, vol. 49, no. 4, pp. 297–298, Feb. 2013.

[122] G. N. Suo, "Low Loss tunable superconducting dual-mode filter at L-band using semiconductor varactors," *IEEE Microw. Wireless Compon. Lett.*, vol. 24, no. 3, pp. 170–172, Mar. 2014.

[123] Z. Y. Yin, "An HTS filter subsystem for 800 MHz mobile communication system," *Int. J. Mod. Phys. B*, vol. 19, no. 1–3, pp. 419–422, Jan. 2005.

[124] Z. S. Yin, "Field trial of an HTS filter system on a CDMA base station," *Chin. Sci. Bull.*, vol. 52, no. 2, pp. 171–174, Jan. 2007.

[125] B. Wei, "Field test of HTS receivers on CDMA demonstration cluster in China," *Chin. Sci. Bull.*, vol. 54, no. 4, pp. 612–615, Feb. 2007.

[126] Y. H. Wang *et al.*, "A narrow band dual mode HTS patch filter with high power capability," *IEEE Microw. Wireless Compon. Lett.*, vol. 19, no. 7, pp. 449–451, Jul. 2009.

[127] X. Q. Zhang *et al.*, "Development of a HTS transceiver sub-system for 3G mobile communication TD-SCDMA base station," *Supercond. Sci. Technol.*, vol. 23, no. 2, p. 025007, Feb. 2010.

[128] C. Li *et al.*, "A high-performance ultra-narrow bandpass HTS filter and its application in a wind-profiler radar system," *Supercond. Sci. Technol.*, vol. 19, no. 5, pp. S398–S402, May 2006.

[129] Q. Zhang *et al.*, "A HTS bandpass filter for a meteorological radar system and its field tests," *IEEE Trans. Appl. Supercond.*, vol. 17, no. 2, pp. 922–925, Jun. 2007.

[130] C. Li *et al.*, "Recent progress of HTS microwave applications in satellite receiver, meteorological radar, mobile communication and radio astronomy," *J. Supercond. Novel Magn.*, vol. 26, no. 5, pp. 1843–1848, May 2013.

[131] L. Gao *et al.*, "A 23 GHz high-temperature superconducting microstrip filter for radio astronomy," *Chin. Sci. Bull.*, vol. 54, no. 19, pp. 3485–3488, Oct. 2009.

[132] J. Huang *et al.*, "Space qualification mechanical tests of HTS filters for satellite applications," *Chin. Sci. Bull.*, vol. 52, no. 13, pp. 1771–1775, Jul. 2007.

[133] Y. Wu, L. Sun *et al.*, "Developments of microwave HTS based devices and subsystems for applications in civilian satellite," in *Proc. 8th Int. Kharkov Symp. Phys. Eng. Microw., Millim. Submillim. Waves*, 2013, pp. 46–51, invited talk.